ORIGINAL CONTRIBUTION

Fabrice Carnal
Abohachem Laguecir
Serge Stoll
Abohachem Laguecir

Simulations and scattering functions of polyelectrolyte – macroion complexes

F. Carnal · A. Laguecir · S. Stoll (✉)
A. Laguecir (✉)
Analytical and Biophysical Environmental
Chemistry (CABE), Department of
Inorganic, Analytical and Applied
Chemistry, Sciences II,
University of Geneva,
30 quai E. Ansermet, 1211 Geneva 4,
Switzerland
E-mail: serge.stoll@cabe.unige.ch
Tel.: +41-22-3796427
Fax: +41-22-3796069
E-mail:
abohachem.laguecir@cabe.unige.ch
Tel.: +41-22-3796427
Fax: +41-22-3796069

Abstract Using Monte Carlo simulations of complex formation between a polyelectrolyte chain and an oppositely charged macroion, we calculated the scattering function of the polyelectrolyte chain. We investigated the case of the isolated polyelectrolyte chain and studied the effect and influence of key parameters such as the ionic concentration of the solution, polyelectrolyte length and intrinsic rigidity on the scattering function. Then, we focused on the polyelectrolyte–macroion complex by calculating the structure factor $S(q)$ of the adsorbed polyelectrolyte chain. Typical conformations ranging from coils, extended chains to solenoids are revealed and the corresponding $S(q)$ analysed. The effects of ionic concentration, chain length and intrinsic rigidity and relative size ratio between the polyelectrolyte and the macroion are investigated. Important effects on the structure factor of the adsorbed polyelectrolyte are observed when the macroion is partially or totally wrapped by the polyelectrolyte. Distance correlations between the polyelectrolyte monomer positions at the surface of the macroion induce the formation of peaks in the fractal regime of $S(q)$. For semiflexible chains, when solenoid conformations are observed, the position of the peaks in the fractal regime corresponds directly to the separation distance between the turns. The formation of a protruding tail in solution is also observed through the formation in the fractal regime of a linear domain.

Keywords Polyelectrolyte–macroion complexes · Structure factor · Monte Carlo simulations

Introduction

The complexation of polyelectrolyte chains with oppositely charged species has recently attracted much attention, because of their important potential applications in nanoscience, environmental chemistry and biology [1, 2, 3, 4, 5, 6]. Polyelectrolyte chains are usually associated with a large range of compounds, including oppositely charged polymers, colloids (inorganic particles, surfactant micelles) and biomacromolecules (proteins, DNA). An example is the DNA–histone complexation which is expected to control the packing of DNA in living cells [7, 8]. Also applications in the field of water treatment in which a colloidal suspension must be destabilized by adsorbed charged polymers to produce clear water are important and a better understanding of these complexes can give hints how to control the destabilization of suspended colloids and promote the rational use of polymeric flocculants [9, 10, 11]. The long-range attractive and/or repulsive character of electrostatic interactions between the charged species, solution chemistry, surface chemistry, geometry and concentration of both polyelectrolytes and particles, but also competitive adsorption, overcharging processes,

etc., give polyelectrolyte–colloid mixtures specific properties. Nonetheless, so far, little is known of the rational use of polyelectrolytes with oppositely charged colloids and the polyelectrolyte-colloid structures are partially understood.

Theoretically, the interactions between oppositely charged macromolecules and colloids (also referred to as macroions) and the resulting structures (complexes) have been the focus of several studies using computational or analytical approaches, and different levels of approximations and models to represent the polyelectrolyte chain and the colloidal particle have been proposed. Most of the studies assume weakly charged objects attracted via standard electrostatics, and consider an explicit or implicit counterion and/or coion description. The complexes that have been investigated most extensively during the past few years are those made from one of polyelectrolyte and one macroion [12, 13, 14, 15, 16]. Some studies also discuss the interactions between two macroions in the presence of one or more polyelectrolyte chains [17, 18, 19, 20]. Netz and Joanny [21, 22] provided a full complexation phase diagram for a semiflexible polyelectrolyte chain model in the presence of an oppositely charged sphere. Both the effects of added salt and chain stiffness were taken into account. They demonstrated that for intermediate salt concentration and high sphere charge, a strongly bound complex, where the polymer completely wraps around the sphere, is obtained and that the low-salt regime is dominated by monomer–monomer repulsions leading to a characteristic hump shape where the polymer partially wraps around the sphere with two polymer arms extended parallel and in opposite directions from the sphere. In the high-salt regime, they suggested that the polymer partially wraps the sphere. Hence, the complexation between a semiflexible polyelectrolyte and an oppositely charged macroion leads to a multitude of structures ranging from tight complexes with the chain wrapped around the macroion to open multileafed rosettelike complexes as described by Schiessel [23]. Using a scaling theory, he provided a complete diagram of states and investigated the transition between the two limits of high and low ionic strength. The binding of one semiflexible polyelectrolyte onto an oppositely charged sphere, using parameters appropriate for DNA–histone complexes was studied numerically by Kunze and Netz [24]. They found complete wrapping for intermediate salt concentration, discontinuous dewrapping for high salt concentration and multiple conformational transition for low salt concentration in agreement with experiments.

Experimental investigations dealing with the determination of the structure of complexes obtained from polyelectrolyte and oppositely charged particles are still few. Dubin and coworkers investigated the effects of added salt on coacervation in systems composed of strong cationic polymers and oppositely charged micelles. The complexation between ferrihaemoglobin and three polyelectrolytes was considered to get an insight into the role of polyelectrolyte charge density and sign [25]. The complex formation between poly(acrylic-acid) and cationic–nonionic mixed micelles to study the effect of pH, ionic concentration on electrostatic interactions and hydrogen bonding was also investigated [26]. Critical conditions for binding of dimethyldodecylamine oxide micelles to polyanions of variable charge density versus pH and ionic concentration were also reported, showing that the required critical surface charge density of the micelles necessary for adsorption was proportional to the inverse Debye screening length κ [27]. Berret et al. [28] reported the scattering properties of colloidal complexes made from block copolymers and surfactants. Combining dynamical light scattering and small-angle neutron scattering (SANS), they demonstrated that in some conditions the colloidal complexes reveal an original core–shell microstructure. They also reported a comparison between SANS, cryogenic transmission electron microscopy and Monte Carlo simulations. The agreement between the model and the data was found to be remarkable and allowed them to conclude that the structure peak observed in the neutron scattering intensity plots was associated with the hard-sphere interactions between micelles in the core.

Monte Carlo simulations have corroborated experimental and theoretical results. Chain flexibility, linear charge density and micelle radius were considered by Wallin, Linse and Akinchina [29, 30] in investigations of the behaviour of sphere–chain complexes. The complexation between a linear flexible polyelectrolyte and several oppositely charged macroions was recently examined by Jonsson and Linse [31, 32] with focus on the effect of linear charge density, chain length, macroion charge and chain flexibility. Composition, structure and thermodynamic properties of the complexes were obtained and the overcharging issue and location of small ions investigated. Dzubiella et al. [33] concentrated on the complex formed by one spherical colloid and one polyelectrolyte as a whole and investigated its polarizability. They observed that the polarizability is large for short chains and small electrical fields and shows non-monotonic behaviour with the chain length at fixed charge density.

Owing to the important potential of computer simulations to provide qualitative and quantitative means of understanding the factors that could influence polyelectrolyte–particle interactions and to investigate the structure of the complexes, we used a Monte Carlo approach to get an insight into the determination and interpretation of the scattering curves of polyelectrolyte–colloid complexes. These curves are expected to provide important and useful information for experimental investigations. A flexible, a semiflexible and a rigid polyelectrolyte

with the presence of small oppositely charged particles were investigated. As the ionic concentration is expected, via screening effects, to play a key role in controlling both chain conformation (via the electrostatic persistence length) and polyelectrolyte–particle interaction energy we also focussed on it. Recently we described in detail the complex formation between a charged colloidal particle and an oppositely charged polyelectrolyte [34, 35, 36] and the phase diagrams we obtained are partly used here to calculate the scattering functions. The polyelectrolyte–particle complex is investigated here with special attention on the effect of the particle size, chain length and salt concentration.

Monte Carlo simulations

Polyelectrolyte chains are represented, using a coarse-grained approach, as a succession of N freely jointed hard spheres, each sphere being considered as a physical monomer with a radius σ_m equal to 3.57 Å and a negative charge equal to -1 on its centre. The chain is considered as a strong polyelectrolyte and the fraction of ionized monomers f is set to 1. The bond length between two monomers is constant and equal to the Bjerrum length $l_B = 7.14$ Å. The macroion is represented as an impenetrable and uniformly charged sphere with a radius σ_p. The macroion surface charge is assumed to result from the point charge located at its centre which is adjusted so as to fix the surface charge density to $+100$ mC m^{-2}, which is representative of values observed for natural inorganic particles at neutral pH. The solvent is treated as a dielectric medium with a relative dielectric permittivity constant ϵ_r taken as that of water at 298 K, i.e. 78. The total energy E_{tot} ($k_B T$ units) for a given conformation is the sum of repulsive electrostatic interactions between monomers and attractive electrostatic interactions between the chain and the macroion. A torsional energetic term is also included to consider a semiflexible polyelectrolyte (such as DNA, polysaccharides and synthetic polymers having an intrinsic persistence length).

All pairs of charged monomers within the polyelectrolyte interact with each other via a screened Debye–Hückel long-range potential,

$$u_{el}(r_{ij}) = \frac{z_i z_j e^2}{4\pi\varepsilon_r\varepsilon_0 r_{ij}} \exp\left(-\kappa r_{ij}\right), \tag{1}$$

where z_i represents the amount of charge on unit i and r_{ij} the distance between the centres of two monomers, while monomers interact with the particle according to a Verwey–Overbeek potential,

$$u'_{el}(r_{ij}) = \frac{z_i z_j e^2}{4\pi\varepsilon_r\varepsilon_0 r_{ij}} \cdot \frac{\exp\left[-\kappa\left(r_{ij} - \sigma_p\right)\right]}{1 + \kappa\sigma_p}. \tag{2}$$

Free ions are not included explicitly in the simulations but their overall effects on monomer–monomer and monomer–particle interactions are described via the dependence of the inverse Debye screening length κ (per metre) on the electrolyte concentration. All pairwise interactions between the monomers and between the monomers and the particle are calculated without taking into account cutoff distances. The intrinsic polyelectrolyte chain stiffness is adjusted with a square-potential with variable amplitude to vary its strength. This gives the total bending energy

$$E_{tor} = \sum_{i=2}^{N} k_{ang}(\alpha_i - \alpha_0)^2, \tag{3}$$

where $\alpha_0 = 180°$ and α_i represents the angle achieved by three consecutive monomers $i-1$, i and $i+1$. k_{ang} (in units of $k_B T$ per degree squared) defines the strength of the angular potential or chain stiffness. Fully flexible chains (but with excluded volume) are achieved when $k_{ang} = 0$.

Monte Carlo simulations were performed according to the Metropolis algorithm in the canonical ensemble. Several million successive "trial" chain configurations were generated to obtain a reasonable sampling of low-energy conformations. To investigate the formation of polyelectrolyte-macroion complexes, the central monomer of the chain is initially placed at the centre of a large three-dimensional spherical box and the macroion is randomly placed in the cell. The polyelectrolyte and the oppositely charged macroion are then allowed to move (random motion is used to move the macroion). A detailed description of the elementary movements and efficiency is given in Ref. [37]. It should be noted here that the chain has the possibility to diffuse further away and leave the macroion surface during a simulation run if the entropy loss of the chain is not balanced by the adsorption energy.

Scattering function

SANS and small-angle X-ray scattering techniques are usually used to determine the structure and dimensions of fractal aggregates [38, 39] and polymer chains [40, 41, 42]. Considering an aggregate composed of a large number N of identical monomers of diameter r_0 the scattered intensity $I(q)$ can be expressed by the double sum over the positions $\mathbf{r}_i$ of the monomer centres: $I(q) = I_0 \sum_{i=1}^{N} \sum_{j=1}^{N} e^{i\mathbf{q}\cdot(\mathbf{r}_i - \mathbf{r}_j)}$, where I_0 is the scattering intensity for an isolated monomer (form factor) and q is the modulus of the scattering wave vector $\mathbf{q}$ given by $q = \frac{4\pi}{\lambda}\sin\frac{\theta}{2}$, where λ is the wavelength of the incident beam and θ the scattering angle. Insofar as values of q^{-1} are larger than the size of a monomer, I_0 can be regarded as independent of q. The calculation of the scattering

intensity is done according to the following expressions [39, 43]:

–For the scattered intensity $I(q)$:

$$I(q) = N \cdot S(q) \cdot P(q), \qquad (4)$$

where N is the number of particles (in our case it corresponds to the total number of monomers of the polyelectrolyte chain).

–For the scattering function or structure factor $S(q)$:

$$S(q) = 1 + \frac{1}{N} \sum_{i \neq j} \frac{\sin q \cdot r_{ij}}{q \cdot r_{ij}}, \qquad (5)$$

with $S(0) = N$ and $S(\infty) = 1$, according to renormalization conditions.

–For the form factor of the spherical monomer $P(q)$:

$$P(q) = v^2 \left(3 \frac{\sin (q/2) - (q/2) \cos (q/2)}{(q/2)^3} \right)^2, \qquad (6)$$

where v represents the volume of the elementary monomer (sphere of diameter $r_0 = 2\sigma_m$):

$$v = \frac{\pi}{6} r_0^3.$$

As shown in Fig. 1, three regimes for the scattering function $I(q)$ can be defined:

1. At low q $(q^{-1} \gg R_g)$, in the Guinier regime, the intensity is proportional to an expression which contains the gyration radius R_g: $\frac{I(q)}{I_0} \approx N^2 \exp \left(\frac{-q^2 R_g^2}{3} \right)$. A plot of the intensity as a function of q on a log–log scale yields the radius of gyration of the object.
2. At intermediate q values, when $r_0 \ll q^{-1} \ll R_g$, the rate of decay is determined by the dimensionality of the
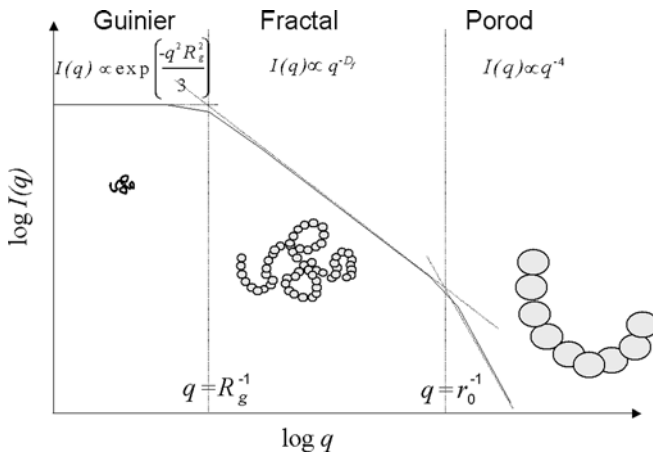

Fig. 1 Schematic representation of the scattered intensity $I(q)$ versus the wave vector q (log–log scale) for a fractal structure. Three modes (*Guinier*, *fractal* and *Porod*) characterize the structure at different scales. The fractal regime is achieved when $r_0 \leq q^{-1} \leq R_g$

structure: linear structures yield a q^{-1} decay, platelets q^{-2}, and dense structures q^{-4}. Intermediate exponents are obtained with fractal structures: fractal objects with fractal dimensions D_f between 1 and 3 are given by q^{-D_f}.
3. When $q^{-1} \ll r_0$, in the Porod regime, a lower scale than the size of the monomer is probed. The surface fractal dimension is 2 for an elementary particle, and it results from the expression of Bale and Schmidt $[I(q) \propto q^{D_s - 6}]$ [44] that the slope shall be equal to –4.

Isolated chain

Influence of the ionic concentration

The ionic concentration C_i is an important parameter which controls the intensity of the electrostatic repulsions between the monomers. Equilibrated conformations of flexible and semiflexible polyelectrolytes ($k_{ang} = 0$ and 0.01 $k_B T$ deg^{-2}) with the corresponding chain scattering functions are presented in Table 1. The ionic concentration ranges from $C_i = 0$ M ($\kappa^{-1} \rightarrow \infty$) to 0.01 M ($\kappa^{-1} = 30$ Å), 0.1 M ($\kappa^{-1} = 9.6$ Å) and 1 M ($\kappa^{-1} = 3$ Å) and the chain length N is equal to 200 monomers. It is important to note here that the case of 0 M is a particular and theoretical situation owing to the fact that charge neutrality according to the model (implicit treatment of the salt) is not guaranteed in all situations. Globally, by decreasing the ionic concentration, extended structures are achieved to minimize the energy of the chain. Extended does not mean a straight pole, but rather a highly oriented object presenting local fluctuations in the monomer positions. When screening increases, isolated polyelectrolytes become less stretched and local correlations between monomers result in the formation of peaks in the scattering function. This is particularly observed at $C_i = 0.1$ M and $k_{ang} = 0.01$ $k_B T$ deg^{-2} where the peak at $q = 0.0224$ Å^{-1} (319 Å) is representative of the correlation distance between the two parallel arms. In the following, q will represent the dimensionless wave vector with q $= q \cdot r_0$. Hence the peak at q $= 1$ Å^{-1} represents the diameter of the monomers that is 7.14 Å.

In Fig. 2, the chain fractal dimension D_f of an isolated flexible polyelectrolyte chain ($N = 200$) is presented with respect to the Debye length κ^{-1}. The fractal dimensions are obtained by calculating the slope of the scattering intensity $I(q) \propto q^{-D_f}$ in the fractal regime. When κ^{-1} increases, i.e. when C_i decreases, the fractal dimension of the chain decreases from the self-avoiding-walk value ($D_f = 1.66$ [45]) to a plateau value which is close to the limit for the rodlike structures ($D_f = 1$). This limit is never reached because of the thermal fluctuations

Table 1 Isolated chain scattering functions $S(q)$ and corresponding snapshots of equilibrated conformations for an isolated polyelectrolyte chain ($N=200$). Two different intrinsic chain rigidities (flexible chain, $k_{ang}=0\ k_B T\ \mathrm{deg}^{-2}$, and semiflexible chain,- $k_{ang}=0.01\ k_B T\ \mathrm{deg}^{-2}$) at various ionic strengths are presented

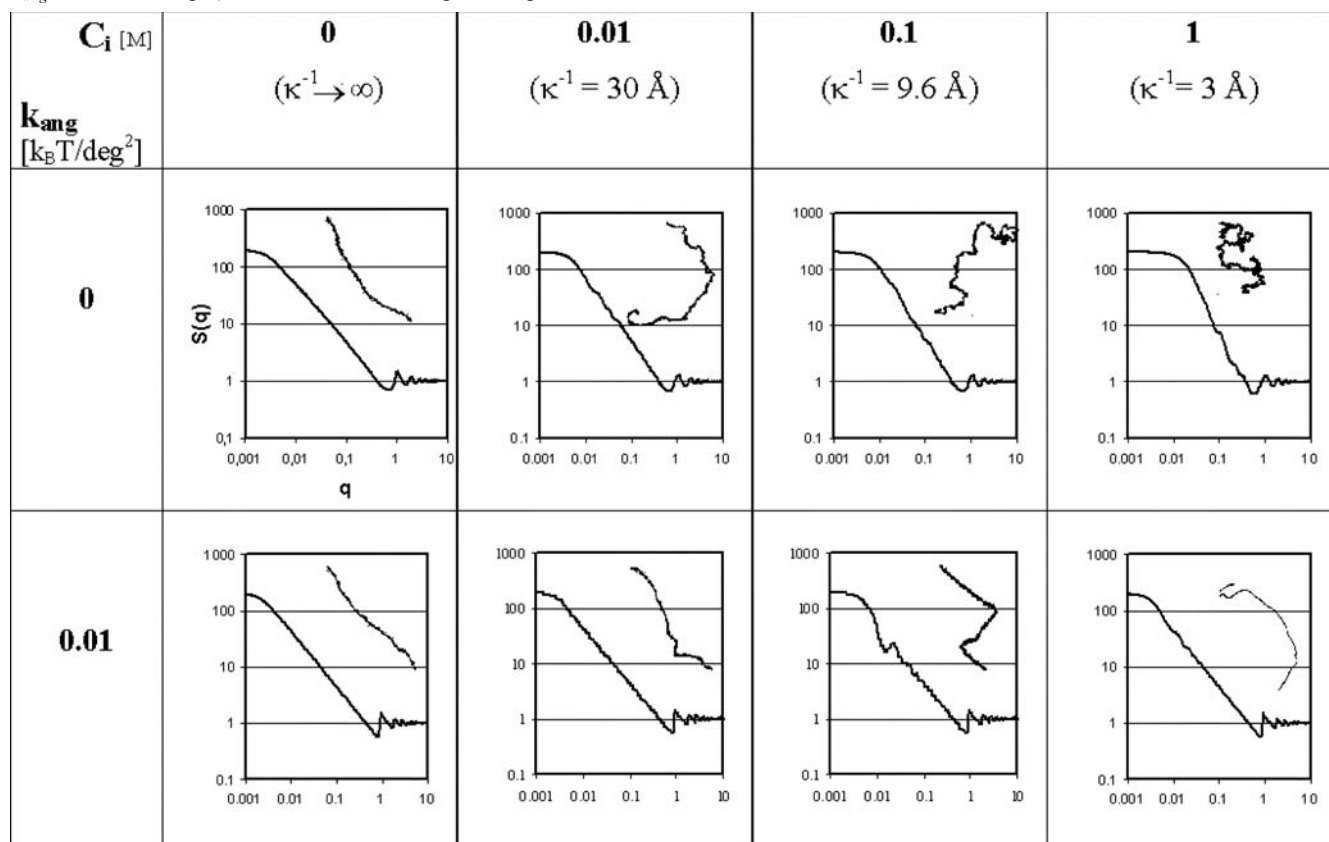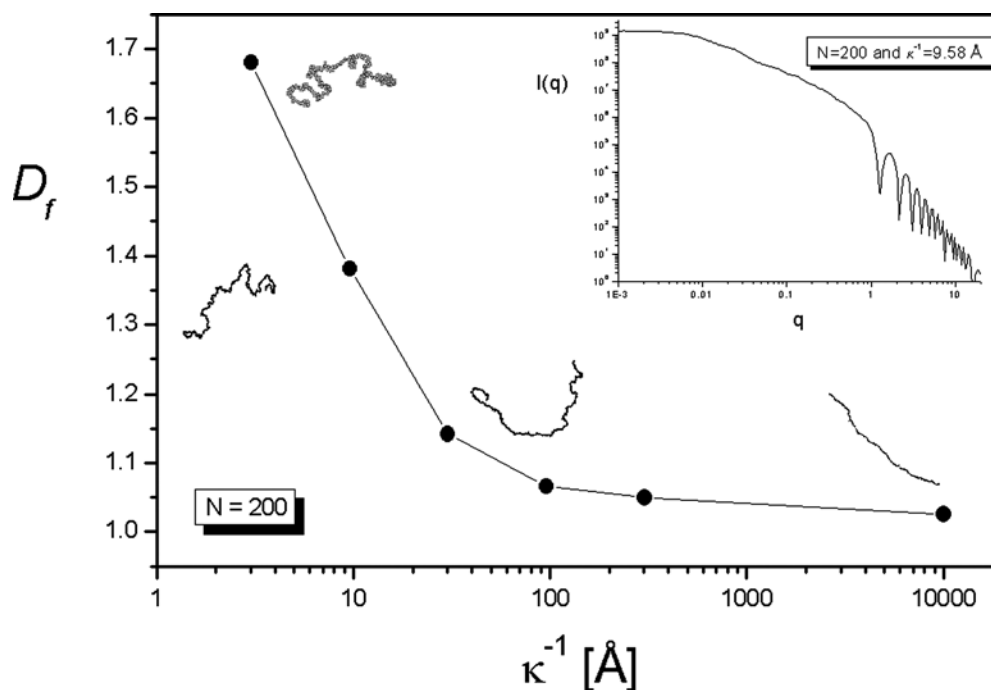| C_i [M] k_{ang} [$k_B T/\mathrm{deg}^2$]	0 ($\kappa^{-1}\rightarrow\infty$)	0.01 ($\kappa^{-1}=30$ Å)	0.1 ($\kappa^{-1}=9.6$ Å)	1 ($\kappa^{-1}=3$ Å)
0				
0.01				

Fig. 2 Chain fractal dimension D_f of isolated flexible polyelectrolyte chains ($N=200$) versus the Debye length κ^{-1}. In the fractal regime, the scattered intensity is related to the monomer–monomer distance correlations, such as $I(q)\propto q^{-D_f}$. The *inset* represents a typical decay of the simulated scattering intensity $I(q)$
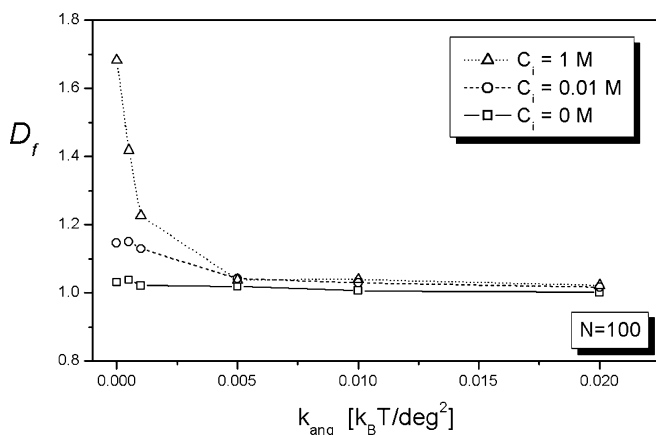
Fig. 3 Chain fractal dimension D_f of an isolated polyelectrolyte chain ($N = 100$) versus the intrinsic chain rigidity k_{ang} at different ionic strengths

causing local chain deformation within the polymer chain. In the inset of Fig. 2, the scattered intensity $I(q)$ of a polyelectrolyte is presented using the expression given by Eq. (4).

Influence of the chain rigidity

When the chain stiffness is set to $k_{ang} = 0.01\ k_B T\ \mathrm{deg}^{-2}$, chain conformations are more extended. It is worth noting that the increase of intrinsic stiffness locally destroys a large amount of chain entropy and results in the formation of rigid domains connected to each other by flexible bonds or kinks (see Table 1, $C_i = 0.1$ M and $k_{ang} = 0.01\ k_B T\ \mathrm{deg}^{-2}$). From this it can be deduced that electrostatic interactions (which control the electrostatic persistence length) and intrinsic stiffness (which controls the intrinsic persistence length) influence each other but at different scales. Although long-range electrostatic repulsions have full effects when $C_i = 0$ M, it is demonstrated here that it is still possible to increase the polyelectrolyte dimensions through local geometric constraints.

In Fig. 3, chain fractal dimensions D_f of isolated polyelectrolyte chains ($N = 100$) are presented versus the intrinsic chain rigidity k_{ang} and at different ionic strengths. When k_{ang} increases, D_f decreases until a plateau value which is almost the limit for the rodlike structures. By decreasing C_i, the plateau value is significantly shifted to a smaller value of D_f, meaning that both electrostatics and intrinsic rigidity are required to achieve straight poles.

Complex formation with flexible chains

In Table 2, structure factors $S(q)$ and the corresponding equilibrated conformations of the complexes are presented as a function of C_i and N to get insight into the role of the chain length on $S(q)$ and to derive structural maps. It should be noted that extended polymer chain conformations appear smaller than their actual size since they have been reduced in size. The size ratio between the macroion and monomer diameter has a constant value of 10.

When the polyelectrolyte is adsorbed at the macroion surface, its conformation is different from its conformation in solution because of its adsorption on a curved surface. When the chain contour length is small, the chain can fully spread on the surface with dimensions close to its dimensions in a free solution, whereas when the chain length is increased to $N = 100$, the polyelectrolyte continuously wraps around the macroion to optimize the number of contacts (charge neutralization is achieved at $N = 100$). The conformation of the polymer is here fully dictated by the macroion size and is subject to the highest level of deformation. By increasing further the chain length, the electrostatic excluded volume of the monomers prevents any additional monomer adsorption on the surface and provokes the formation of an extended tail in solution (in addition overcharging of the macroion is also observed: more information about that issue can be found in Ref. [35]).

Conformational changes can also be observed by the analysis of the chain scattering functions. For $N = 25$ and $C_i = 0$ M, a linear power-law decay of $S(q)$ is observed, meaning that spatial correlations between the monomers are small. When chain length increases, peaks appear in the fractal regime because of correlations between the monomers at the macroion surface. For example, when $N = 100$ and $C_i = 0$ M, the largest peak at $q = 0.1\ \text{Å}^{-1}$ corresponds exactly to the diameter of the macroion, i.e. 71.4 Å. When the ionic concentration is increased to 0.3 M, the peak becomes less prominent because of the formation of loops and tails. When $N = 160$ and $C_i = 0$ M, the formation of the extended tail is also observed through the emergence of a second slope in the fractal regime—and a decrease of $S(q)$ at $q = 0.1\ \text{Å}^{-1}$. The slope of $S(q)$ corresponding to the extended tail is observed at a distance of 238 and 1,020 Å ($q = 0.03$ and $0.007\ \text{Å}^{-1}$), while the slope corresponding to the polyelectrolyte adsorbed on the macroion is between 11.9 and 238 Å ($q = 0.6$ and $0.03\ \text{Å}^{-1}$, respectively). The slope corresponding to the tail is lower because of the rodlike character of the protruding tail.

Complex formation with a semiflexible chain

In this section, we investigate the effect of chain rigidity on $S(q)$. Table 3 represents equilibrated conformations of polyelectrolyte–macroion complexes with respect to ionic concentration and intrinsic rigidity k_{ang}.

Table 2 Chain scattering functions $S(q)$ and corresponding snapshots of equilibrated conformations of polyelectrolyte–macroion complexes. The influence of the polyelectrolyte length and ionic concentration is investigated

C_i [M] \ N	0	0.01	0.1	0.3
25				
100				
160				
200				
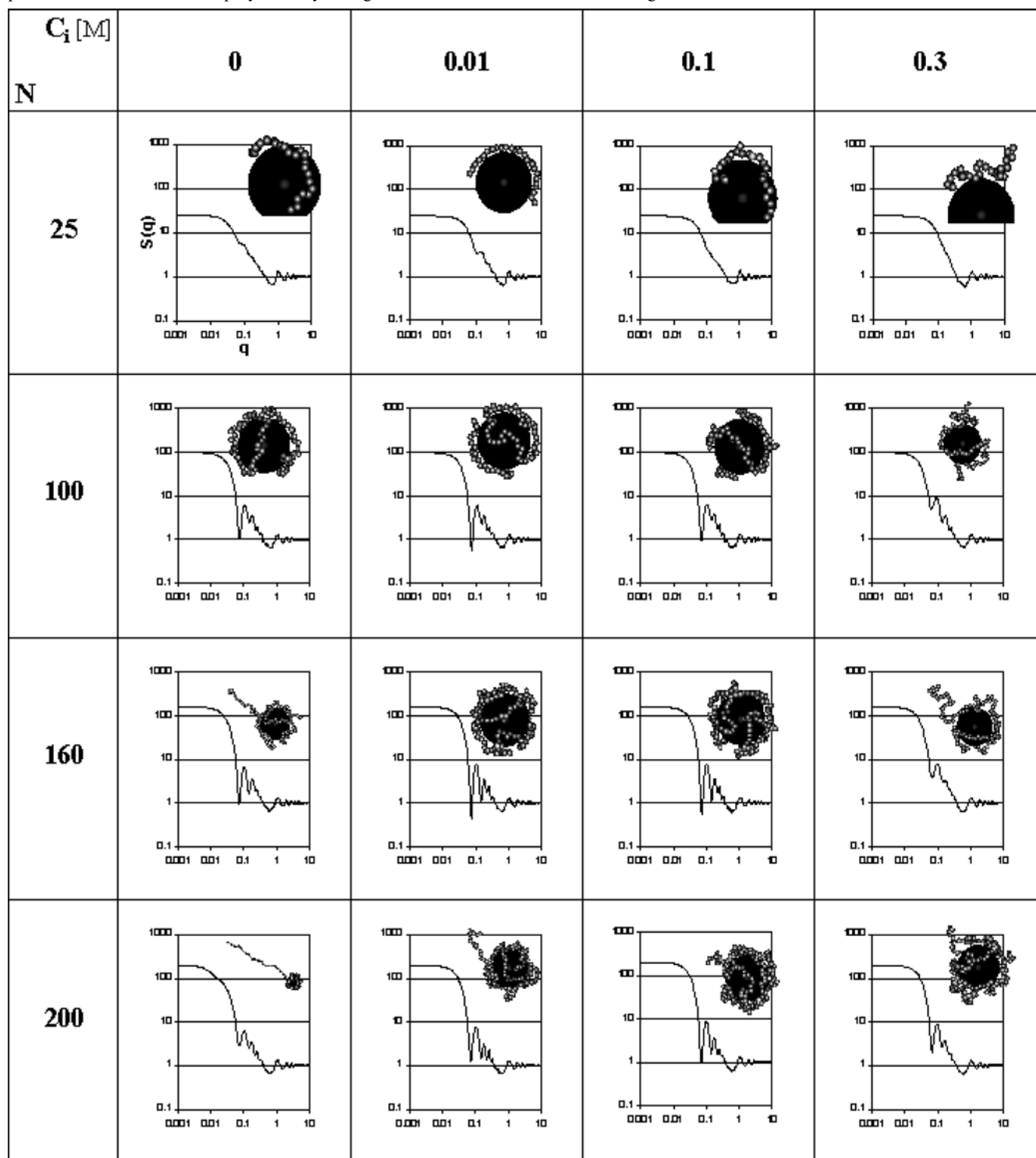
For flexible chains ($k_{ang} < 0.005$ $k_B T$ deg^{-2}), "tennis ball" conformations are achieved at the macroion surface, whereas when rigid chains are considered ($k_{ang} \geq 0.005$ $k_B T$ deg^{-2}), one can observe solenoid conformations at medium and low ionic concentration ($C_i = 0$–0.1 M). According to the contour chain length

Table 3 Chain scattering functions $S(q)$ and corresponding snapshots of equilibrated conformations of polyelectrolyte–macroion complexes. The influence of the polyelectrolyte intrinsic rigidity and ionic concentration is investigated ($N = 100$)

C_i [M] k_{ang} [$k_B T$/deg^2]	0	0.01	0.1	0.3
0				
0.005				
0.01				
0.02				
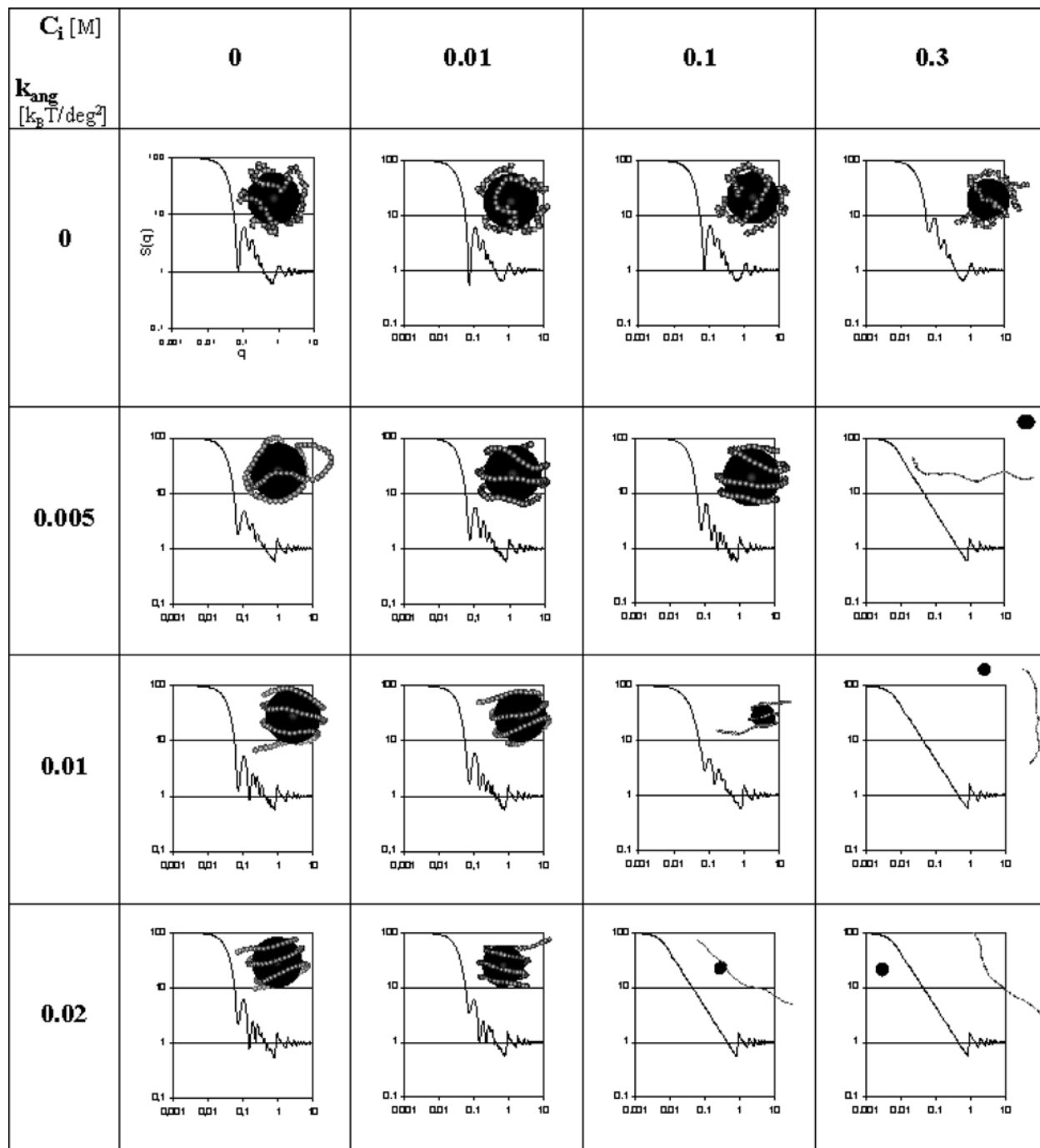
and particle size ratio, the solenoid achieves approximately three turns around the macroion. Both the strong electrostatic repulsions between the neighbouring turns and intrinsic chain rigidity keep the turns parallel to each other as well as a constant distance between them. When $k_{ang} \geq 0.005\ k_B T\ \mathrm{deg}^{-2}$, and with increasing C_i, the polyelectrolyte starts to leave the surface by winding off. Extended tails in solution are formed concomitantly with a decrease in the number of turns of the solenoid. By increasing further the ionic concentration or chain intrinsic flexibility, the polyelectrolyte becomes tangential to the macroion surface with dimensions close to its free unperturbed dimensions.

Fig. 4 Superposition of two adsorbed polyelectrolyte chain scattering functions for semiflexible chains ($k_{ang} = 0$ $k_B T$ deg^{-2}) and semiflexible chains ($k_{ang} = 0.02$ $k_B T$ deg^{-2})
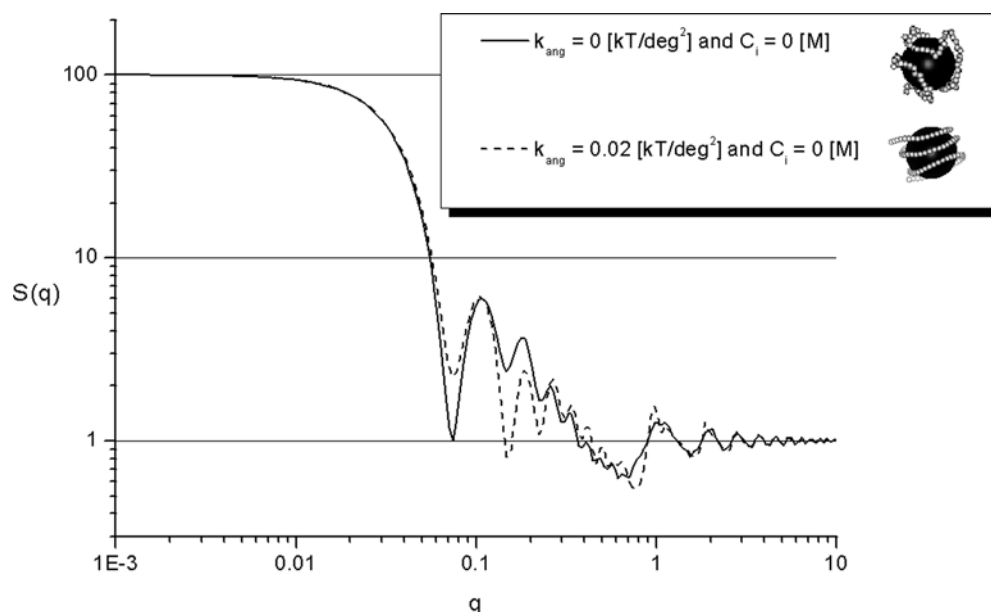
The scattering function is also sensitive to the value of k_{ang} and the formation of the solenoids can be revealed from the analysis of chain scattering functions. When complexes are formed, typical peaks at distances of 7.14 and 71.4 Å, which correspond to the correlation between the monomers along the chains and between the monomers adsorbed at the surface of the macroion, are observed. It should be mentioned that the intensity of the peak at 71.4 Å is directly linked to the number of monomers in the trains. Hence when tangent conformations are achieved such a peak is not observed. When strong complexes are formed (tangent conformations are not considered now), a series of peaks emerges in the fractal regime. When $k_{ang} = 0$ $k_B T$ deg^{-2}, the peaks correspond to the correlations existing between the monomers at the surface of the macroion. When $k_{ang} \geq 0.005$ $k_B T$ deg^{-2}, a solenoid conformation appears with approximately three turns around the macroion. This results in an increase of the monomer correlations in the fractal regime; the typical correlation peaks at distances of 7.14 and 71.4 Å are always present, but the peaks are more prominent than in the case of the flexible chain, owing to the formation of an ordered solenoid conformation. The position of the peaks in the fractal regime corresponds directly to the separation distance between the turns. A comparison of two chain scattering function $S(q)$ at $k_{ang} = 0$ and 0.02 $k_B T$ deg^{-2} with $C_i = 0$ M is presented in Fig. 4. A significant difference in the $S(q)$ variation between the two conformations is observed. When $k_{ang} = 0.02$ $k_B T$ deg^{-2}, the correlations between the successive turns are well pronounced and correspond respectively to q = 0.186, i.e. 38 Å, for both adjacent turns and to q = 0.107, i.e. 66 Å, for the external turns. The prominence of these peaks in the fractal regime is expected to decrease with the decrease of the chain length because of the decrease of the correlations between monomers (Table 2, $C_i = 0$ M and $N = 25$). This is also valid when the chain length increases because of the formation of the protruding tails.

Influence of the relative size ratio between the chain and the macroion

Equilibrated conformations of polyelectrolyte–macroion complexes as a function of ionic concentration and relative size ratio between the macroion σ_p and monomer chain σ_m ($\sigma_p / \sigma_m = 5$, 10, 15, 25 and 50, respectively) are presented in Table 4. It can be clearly seen that the polyelectrolyte chain conformation is strongly dependent on the relative sizes of the macroion and ionic concentration. Collapsed, tennis ball and tangent conformations are achieved. When $\sigma_p / \sigma_m < 5$, the extended polyelectrolyte conformation is little affected by the presence of a small macroion (here the macroion can be considered as adsorbed at the polyelectrolyte). By increasing the σ_p / σ_m ratio (by increasing the size of the macroion), the macroion surface becomes large enough to adsorb most of the monomer segments. Maximum deformation is achieved at $\sigma_p / \sigma_m = 10$. Above this size ratio the electrostatic repulsion between the monomers at the macroion surface is not important enough to limit the adsorption process through the formation of an extended tail in solution. By increasing the macroion size further, i.e. when $\sigma_p / \sigma_m \gg 10$, the nearly planar surface limit is approached. In this case, the chain can spread fully on the surface with dimensions close to its dimensions in a free solution.
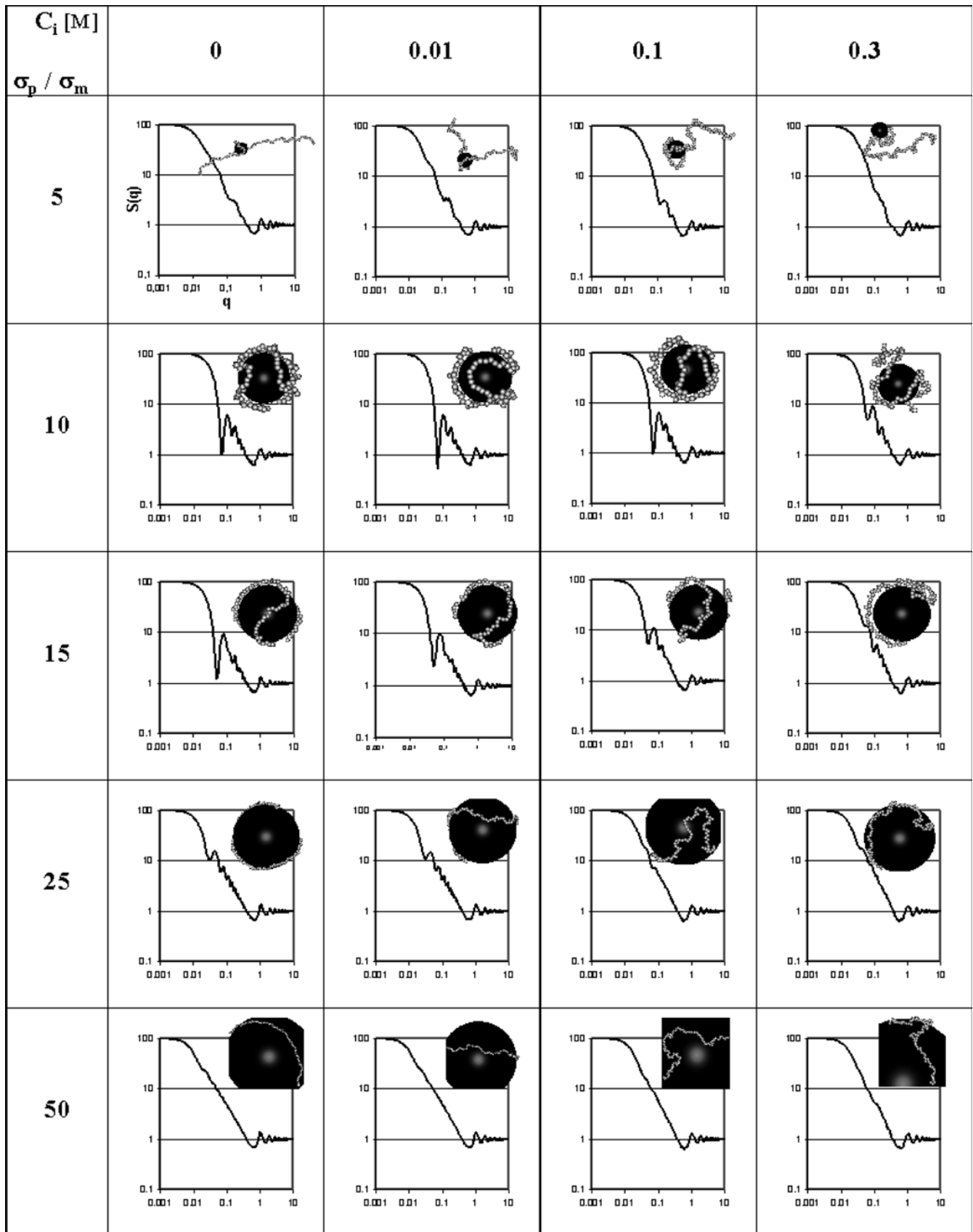
C_i [M] σ_p / σ_m	0	0.01	0.1	0.3
5				
10				
15				
25				
50				

◄

Table 4 Chain scattering functions $S(q)$ and corresponding snapshots of equilibrated conformations of polyelectrolyte–macroion complexes at different relative size ratios σ_p/σ_m between the macroion (σ_p) and the polyelectrolyte chain (σ_m) at various ionic strengths ($N = 100$)

Such observations are corroborated by the analysis of the evolution of the chain scattering functions. When $\sigma_p/\sigma_m = 5$ and $C_i = 0$ M, the fractal regime is almost linear; only one peak is present at 38.39 Å, which corresponds to the diameter of the macroion. The chain is almost linear with approximately one turn around the macroion. By increasing the ionic concentration, since more monomers are expected to be present in the vicinity of the macroion, the peak becomes more pronounced because of the decrease of the monomer–monomer electrostatic repulsions. In the high-salt regime, the slope of $S(q)$ is increased because of the formation of self-avoiding-walk chains, which results in an increase of the polyelectrolyte fractal dimension. When $\sigma_p/\sigma_m \geq 10$, the polyelectrolyte collapses around the macroion again and the characteristic peak related to the monomer correlations between monomer positions and turns at the surface of the macroion are observed. When the size of the macroion increases further, the position of the peak is shifted to the low q values. When $\sigma_p/\sigma_m = 50$, as the conformation of the polyelectrolyte is extended, correlation peaks are reduced and the fractal regime is almost linear.

Conclusion

Using computer simulations, we investigated the complex formation between a polyelectrolyte chain and an oppositely charged macroion. The influence of a large number of parameters was investigated (ionic concentration, intrinsic chain rigidity, polyelectrolyte contour length, size of the macroion) and we demonstrated that complexation leads to a multitude of specific architectures ranging from coils to solenoids with the chain wrapped around the macroion to extended conformations. To bridge the gap between experiments and to allow a direct comparison of scattering functions between simulations and experimental data, the structure factors of the adsorbed (and nonadsorbed) polyelectrolyte chain were calculated. Important effects on the structure factors are observed when the macroion is partially or totally wrapped by the polyelectrolyte. Distance correlations between the monomer positions at the surface of the macroion induce the formation of peaks in the fractal regime. The formation of protruding tails in solution is also observed through the formation in the fractal regime of a linear domain with a slope close to 1.

The simulations reported here are a preliminary step to bridge the gap with experiments. A simple model involving one chain interacting with one particle has been described. It could be extended to more complicated systems involving several chains, macroions as well as to polydisperse systems. We hope the observations made in this study will be particularly useful for the interpretation of experimental data of polyelectrolyte–macroion complexes.

References

1. Flory PJ (1992) Principles of polymer chemistry, Cornell University, Ithaca
2. Xia J, Dubin PL (1994) In: Dubin PL, Bock D (eds) Protein-polyelectrolyte complexes. Springer, Berlin Heidelberg New York
3. Hara M (1993) Polyelectrolytes: sciences and technology Dekker, New York
4. Napper DH (1983) Polymeric stabilization of colloidal dispersions. Academic, New York
5. Finch CA (1996) Industrial water soluble polymers. Royal Society of Chemistry, Cambridge
6. Rädler JO, Koltover I, Salditt T, Safinya CR (1997) Science 275:810
7. Nguyen TT, Shklovskii BI (2000) J Chem Phys 115:7298
8. Gelbart WM, Bruinsma RR, Pincus PA, Parsegian VA (2000) Phys Today 53:38
9. Buffle J, Wilkinson KJ, Stoll S, Fillela M, Zhang J (1998) Environ Sci Technol 32:2887
10. Stoll S, Buffle J (1996) J Colloid Interface Sci 180:548
11. Stoll S, Buffle J (1998) J Colloid Interface Sci 205:290
12. Mateescu EM, Jeppesen C, Pincus PA (1999) Europhys Lett 46:493
13. Feng J, Ruckenstein E (2003) Polymer 44:3141
14. Nguyen TT, Shklovskii BI (2000) Physica A 293:324
15. Welch P, Muthukumar M (2000) Macromolecules 33:6159
16. Gurovitch E, Sens P (1999) Phys Rev Lett 82:339
17. Schiessel H, Bruisma R, Gelbart WM (2001) J Chem Phys 115:7245
18. Akinchina A, Linse P (2002) Macromolecules 35:5183
19. Podgornik R, Akesson T, Jönsson B (1995) J Chem Phys 102:9423
20. Nguyen TT, Shklovskii BI (2001) J Chem Phys 114:5905
21. Netz RR, Joanny JF (1998) Macromolecules 31:5123
22. Netz RR, Joanny JF (1999) Macromolecules 32:9026
23. Schiessel H (2003) Macromolecules 36:3424

24. Kunze KK, Netz RR (2000) Phys Rev Lett 85:4389
25. Xia J, Dubin PL, Kokufuta E, Havel H, Muhoberac BB (1999) Biopolym Field 50:153
26. Yoshida K, Sokhakian S, Dubin PL (1998) J Colloid Interface Sci 205:257
27. Feng XH, Dubin PL, Zhang HW, Kirton GF, Bahadur P, Parotte J (2001) Macromolecules 34:6373
28. Berret JF, Cristobal G, Hervé P, Oberdisse J, Grillo I (2000) J Phys Chem B 104:11689
29. Wallin T, Linse P (1998) J Chem Phys 109:5089
30. Akinchina A, Linse P (2003) J Phys Chem B 107:8011
31. Jonsson M, Linse P (2001) J Chem Phys 115:3406
32. Jonsson M, Linse P (2001) J Chem Phys 115:10975
33. Dzubellia J, Moreira AG, Pincus PA (2003) Macromolecules 36:1741
34. Chodanowski P, Stoll S (2001) J Chem Phys 115:4951
35. Chodanowski P, Stoll S (2001) Macromolecules 34:2320
36. Chodanowski P, Stoll S (2002) Macromolecules 35:9556
37. Chodanowski P, Stoll S (1999) J Chem Phys 111:6069
38. Jullien R, Hasmy A (1995) Phys Rev Lett 74:4003
39. Hasmy A, Foret M, Pelous J, Jullien R (1993) PhysRev B 48:9345
40. Essafi W, Lafuma F, Williams CE (1995) J Phys II 5:1269
41. Borsali R, Rinaudo M, Noirez L (1995) Macromolecules 28:1085
42. Micka U, Holm C, Kremer K (1999) Langmuir 15:4033
43. Kallala M, Jullien R, Cabane B (1992) J Phys II 2:7
44. Bale HD, Schmidt PW (1984) Phys Rev Lett 53:596
45. Stoll S, Dayantis J, Buffle J (1999) Macromol Theory Simul 8:119